Biochemical and Biophysical Research Communications 423 (2012) 289–294

Contents lists available at SciVerse ScienceDirect

Biochemical and Biophysical Research Communications

journal homepage: www.elsevier.com/locate/ybbrc

Mechanistic insights into human pre-mRNA splicing of human ultra-short introns: Potential unusual mechanism identifies G-rich introns

Noriko Sasaki-Haraguchi [a], Makoto K. Shimada [a], Ichiro Taniguchi [b], Mutsuhito Ohno [b], Akila Mayeda [a,*]

[a] Division of Gene Expression Mechanism, Institute for Comprehensive Medical Science, Fujita Health University, Toyoake, Aichi 470-1192, Japan
[b] Institute for Virus Research, Kyoto University, Kyoto 606-8507, Japan

ARTICLE INFO

Article history:
Received 15 May 2012
Available online 26 May 2012

Keywords:
Pre-mRNA splicing
Ultra-short intron
Intronic splicing enhancer
G-rich sequence
U snRNA
Spliceostatin A

ABSTRACT

It is unknown how very short introns (<65 nt; termed 'ultra-short' introns) could be spliced in a massive spliceosome (>2.7 MDa) without steric hindrance. By screening an annotated human transcriptome database (H-InvDB), we identified three model ultra-short introns: the 56-nt intron in the *HNRNPH1* (hnRNP H1) gene, the 49-nt intron in the *NDOR1* (NADPH dependent diflavin oxidoreductase 1) gene, and the 43-nt intron in the *ESRP2* (epithelial splicing regulatory protein 2) gene. We verified that these endogenous ultra-short introns are spliced, and also recapitulated this in cultured cells transfected with the corresponding mini-genes. The splicing of these ultra-short introns was repressed by a splicing inhibitor, spliceostatin A, suggesting that SF3b (a U2 snRNP component) is involved in their splicing processes. The 56-nt intron containing a pyrimidine-rich tract was spliced out in a lariat form, and this splicing was inhibited by the disruption of U1, U2, or U4 snRNA. In contrast, the 49- and 43-nt introns were purine-rich overall without any pyrimidine-rich tract, and these lariat RNAs were not detectable. Remarkably, shared G-rich intronic sequences in the 49- and 43-nt introns were required for their splicing, suggesting that these ultra-short introns may recruit a novel auxiliary splicing mechanism linked to G-rich intronic splicing enhancers.

1. Introduction

The length distributions of vertebrate pre-mRNA introns have a bimodal pattern, e.g., a narrow distribution peaking around ~100 nucleotides (nt) ('short introns') and a broad distribution peaking around ~2000 nt ('long introns') in humans [1,2]. Although intron-definition and exon-definition models have been proposed for the splicing of short and long introns, respectively [3], we do not know much about the exact splicing mechanisms for introns in extra-range below and above of the bimodal distribution. In fact, the mechanism of pre-mRNA spicing has been studied with model pre-mRNAs containing single short introns (100–250 nt), which have been spliced efficiently *in vivo* and *in vitro* (reviewed in [4,5]).

Here, we focus on very short introns in the range below the narrow distribution of the first mode, i.e., less than 65 nt in length, which we designated 'ultra-short introns' (Shimada et al., manuscript in preparation). Early studies showed that a minimum intron length of 78–80 nt is necessary for their splicing [6,7]. However, the real minimum length cannot be inferred from these data because these tested introns were arbitrarily shortened from natural introns, which would eliminate important *cis*-acting elements [8,9]. We carefully screened human genes containing functional ultra-short introns and the splicing of identified three model ultra-short introns (43, 49, and 56 nt) was verified *in vivo* and *in vitro*.

Human nuclear pre-mRNA splicing involves dynamic stepwise reactions in a huge spliceosome, which includes five kinds of U snRNPs and ~170 proteins (reviewed in [5,10]). Essential *cis*-reactive elements in the pre-mRNA; the 5′ splice site, the branch-point sequence, and the 3′ splice site, are simultaneously bound by corresponding *trans*-acting factors, U1 snRNP, U2 snRNP, and $U2AF^{65}$/$U2AF^{35}$, respectively, leading to the initial ATP-dependent formation of the spliceosomal A complex (~2.5 MDa) [11]. Structural analysis by electron microscopy has estimated that the A complex has an asymmetric globular shape, with dimensions of ~26 × 20 × 19.5 nm [11]. Thus, the A complex fully occupies the length of an 85–113-nt linearized RNA (as 1-nt RNA = 0.23 nm; reference [12]), which is about twofold longer than the ultra-short introns we tested (43–56 nt). Therefore, we asked how these three essential splicing signals can be recognized by the corresponding essential factors without steric hindrance.

2. Materials and methods

Full descriptions are provided in the Supplementary Materials and methods.

Abbreviations: SSA, spliceostatin A; PAGE, polyacrylamide gel electrophoresis; ORF, open reading frame; ISE, intronic splicing enhancer; ESE, exonic splicing enhancer.

* Corresponding author. Fax: +81 562 93 8834.
E-mail address: mayeda@fujita-hu.ac.jp (A. Mayeda).

0006-291X/$ - see front matter © 2012 Elsevier Inc. All rights reserved.
http://dx.doi.org/10.1016/j.bbrc.2012.05.112

2.1. Construction of expression plasmids

The expression plasmids for transient transfections of cultured cells were constructed by subcloning the corresponding PCR fragments from the *HNRNPH1, NDOR1, and ESRP2* genes, together with PCR fragments from the pBI-EGFP plasmid, into the pCAGGS vector [13]. These amplified products were subcloned into the pGEM-T Easy vector with the MS2-binding domain fragment from the AdML-M3 plasmid [14,15] for the templates of *in vitro* transcription. PCR amplifications were performed with Blend Taq DNA polymerase and the corresponding DNA primers.

2.2. Transfection of cells and RT–PCR analysis

The indicated human cell lines were transiently transfected with the indicated expression plasmids using Lipofectamine LTX. The transfected cells were incubated for a total of 22 h. Spliceostatin A (SSA) [16] was added 16 h after transfection. Their total cellular RNA was extracted with the PureLink RNA Mini Kit, digested with DNase I, and reverse transcribed using the PrimeScript reverse transcriptase with an oligo-dT primer or specific primers. All the PCR products were analyzed by 5% polyacrylamide gel electrophoresis (PAGE).

2.3. In vitro splicing assays and detection of lariat introns

To prepare [^{32}P] UTP-labeled hnRNP H1, NDOR1, ESRP2, and β-globin pre-mRNAs, *in vitro* transcription with T7 or SP6 RNA polymerase was performed as described previously [17]. The *in vitro* splicing assays were performed as described [17], with the indicated modifications. The selective detection of lariat products by RNase R digestion was performed as described previously [18]. The digested products were analyzed by denaturing 7% PAGE, and visualized using a Bio-imaging Analyzer (Fujix BAS1000, Fujifilm) as described [17].

2.4. Disruption of U snRNAs and splicing assays in Xenopus oocytes

The microinjection of RNA into *Xenopus* oocytes and the preparation of the RNA were performed as described previously[19]. Antisense oligonucleotide directed against U1, U2, or U4 snRNA [20,21] was injected into the *Xenopus* oocyte cytoplasm to disrupt these snRNAs by the endogenous RNase H activity, as described previously [22].

3. Results

3.1. Human ultra-short introns were screened and identified

Using the intronic sequences from the human transcript database (H-InvDB, version 6.0) and the human genome database (NCBI build 36), we derived the pattern of the length distribution of the human introns that are shorter than 945 nt (Fig. 1A, left panel). We observed that the number of human introns increases drastically from 65 nt toward the first mode of the distribution at 83 nt, which is essentially consistent with previous reports [1,2]. Most of these short introns could be spliced by the well-known conventional mechanism because the mechanism was established using short introns in this range, either *in vitro* or in transfected cells. However, we assumed that a considerable number of candidate introns shorter than the 65-nt threshold would not be spliced by the known conventional mechanism, and thus categorized them as 'ultra-short introns' (Fig. 1A, right panel).

There are 190 counts of ultra-short candidate introns shorter than 57 nt, with the terminal GT and AG nucleotides. By removing the candidate sequences that included possible alignment mistakes and varying numbers of tandem repeats, we identified 33 candidate ultra-short introns (Supplementary Table S1). We further screened these ultra-short introns based on their locations in an open reading frame (ORF), the functional identities of their host protein-coding genes, and their conservation in primates, such as the chimpanzee and macaque (Supplementary Materials and methods). In this way, we selected three representative model ultra-short introns: the sixth intron (56 nt) in the hnRNP H1 (*HNRNPH1*) gene (an annotated transcript information in HIT000192494), the twelfth intron (49 nt) in the NADPH-dependent diflavin oxidoreductase-1 (*NDOR1*) gene (HIT000009363), and the sixth intron (43 nt) in the epithelial splicing regulatory protein-2 (*ESRP2*) gene (HIT000008845) (Fig. 1B). There was no specific bias in the positions of the ultra-short introns in their host genes. Remarkably, the shorter two ultra-short introns (49 and 43 nt) do not possess any apparent consensus sequence for branch points, (C/T)TNA(C/T) followed by polypyrimidine tracts, that have been reported in human genes [23].

3.2. Selected human ultra-short introns were spliced in living cells

We checked whether these endogenous ultra-short introns are actually spliced in cultured cells by RT–PCR. The hnRNP H1 pre-mRNA, containing the 56-nt intron, was efficiently spliced. We found distal alternative 3′ splice sites in the 49- and 43-nt introns of the NDOR1 and ESRP2 pre-mRNAs, which generate 76- and 73-nt introns, respectively. These distal 3′ splice sites were used more efficiently than the proximal 3′ splice sites (Fig. 1B, panels for NDOR1 and ESRP2). Especially, a specific inner reverse primer was required to clearly detect the proximal 49-nt NDOR1 intron (Fig. 1B, lower panel of NDOR1). These data confirm that the three model ultra-short introns in the endogenous hnRNP H1, NDOR1, and ESRP2 pre-mRNAs are indeed spliced in cultured cells.

3.3. Splicing factor SF3b is involved in splicing of ultra-short introns

Because the ultra-short introns are too short to be assembled with the known authentic spliceosome, which includes essential factors such as the U1 snRNP, U2 snRNP, and U2AF^{65}/U2AF^{35} in the early step [4], we assumed that their splicing is catalyzed in a more compact spliceosome that lacks the known essential factors.

To test this assumption, we first used the splicing inhibitor, SSA, which interferes with splicing through the specific binding to SF3b (a component of the U2 snRNP) [16]. Human cells were transfected with mini-gene encoding the 56-nt (hnRNP H1), 49-nt (NDOR1), or 43-nt (ESRP2) intron with or without SSA in the culture medium (Fig. 2A). We found that SSA significantly inhibited the splicing of these ultra-short introns, as well as the splicing *via* the distal alternative 3′ splice sites of NDOR1 and ESRP2. These data demonstrate that SF3b is not a dispensable splicing factor for these ultra-short introns.

3.4. U1, U2, and U4 snRNPs are required to splice the 56-nt intron

Using the established *Xenopus* oocyte microinjection system, we next tested whether the essential U snRNPs are required for splicing of these ultra-short introns. Each ^{32}P-labeled pre-mRNA containing the 56-nt (hnRNP H1), 49-nt (NDOR1), or 43-nt (ESRP2) intron was microinjected into oocytes of *Xenopus laevis*, together with the control 231-nt adenovirus major late intron (AdML). The 56- and 231-nt introns were efficiently spliced (Fig. 2B, lanes 1, 3), whereas the 49- and 43-nt introns were not spliced (data not shown). Therefore, we could only use the hnRNP H1 pre-mRNA

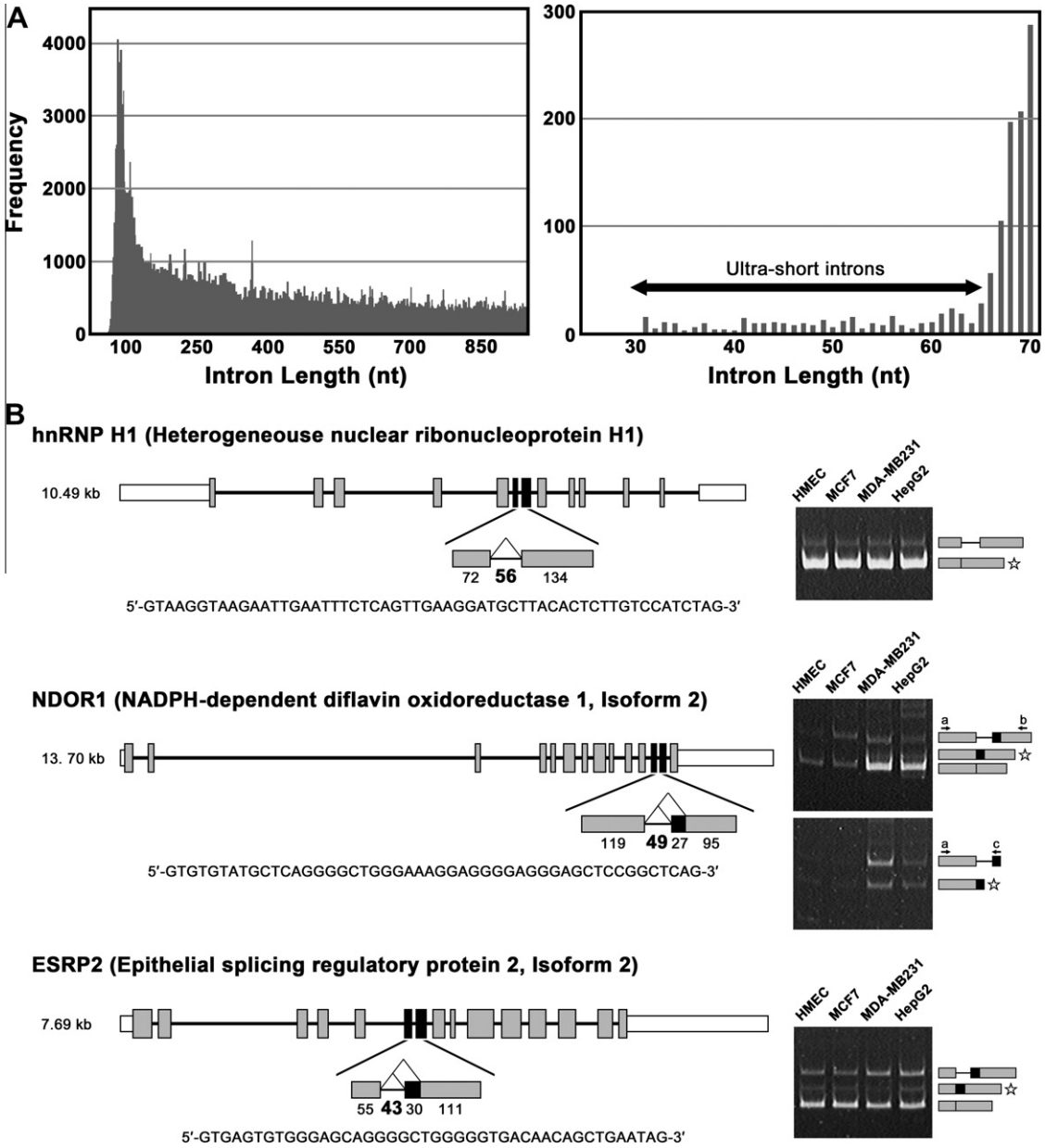

Fig. 1. Human ultra-short introns spliced in cells were identified. (A) The length distribution of human introns was plotted based on data from the human genome and transcriptome. The distributions of intron lengths less than 945 nt (left panel) and less than 70 nt (right panel) are shown. **(B)** The structures of three indicated human genes that contain ultra-short introns (enlarged), and these sequences are shown below. Endogenously spliced 56-nt (hnRNP H1), 49-nt (NDOR1), and 43-nt (ESRP2) introns in the indicated cell lines were detected by RT–PCR and the amplified fragments were analyzed by 5% PAGE (right panels; the stars indicate the spliced products of these ultra-short introns).

(with the 56-nt intron) for the following U snRNP-disruption experiment.

An antisense oligonucleotide-directed degradation of U1, U2, or U4 snRNA in oocytes was performed, and the functional disruption of each U snRNA was monitored by the splicing inhibition of the control AdML pre-mRNA. We found that the disruption of either the U1, U2, or U4 snRNA inhibited the splicing of the hnRNP H1 pre-mRNA (Fig. 2B, lanes 5–10), suggesting that the U1, U2, and U4 snRNAs are required to splice the 56-nt intron.

3.5. In vitro splicing excises the 56-nt intron with a lariat structure

To investigate whether the ultra-short intron is excised as an authentic lariat form, despite its limiting size, we performed *in vitro* splicing and the lariat RNAs generated were analyzed by digestion with RNase R. RNase R, which is an *Escherichia coli* 3′ to 5′ exoribonuclease, thoroughly degrades abundant linear RNA and branched RNA, whereas the loop portion of any lariat RNA remains intact [18].

The pre-mRNAs that included the ultra-short introns (56, 49, and 43 nt) were spliced *in vitro* under varying KCl concentrations (Supplementary Fig. S1). As observed previously [18], when the β-globin pre-mRNA was spliced and the products were digested with RNase R, a discrete band was detected on the PAGE gel, which was the lariat RNA (158 nt) without the 3′ tail derived from the lariat intermediate and the excised lariat intron (Fig. 3, lanes 3, 4). We used this technique to examine whether *in vitro* splicing generates ultra-short introns with a lariat structure. Splicing of the hnRNP H1 pre-mRNA generated a discrete RNase R-resistant band, which was identified as the lariat intron (56 nt) without the 3′ tail (lanes 7, 8;

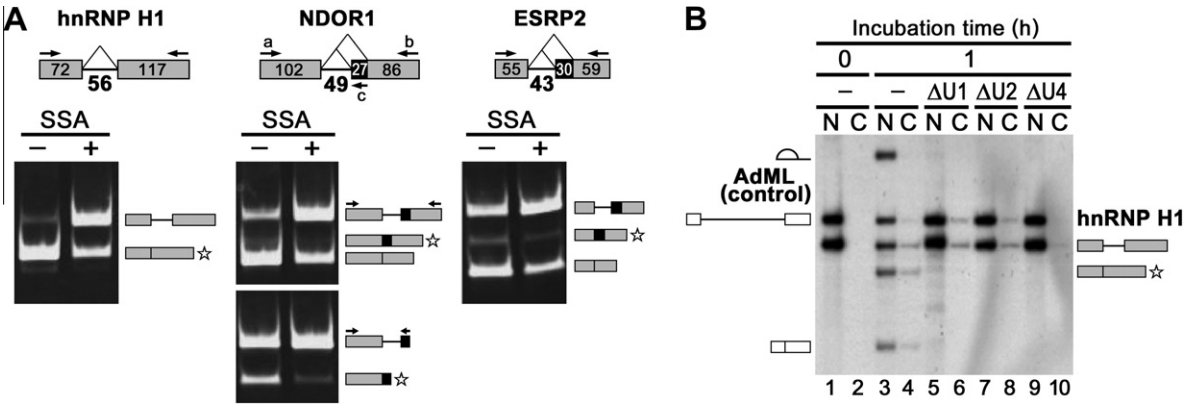

Fig. 2. Splicing in cells and oocytes showed that SF3b is required for all the ultra-short introns and the U snRNPs are required for the 56-nt intron. **(A)** The MDA-MB231 cells were transfected with mini-genes containing the 56-, 49-, and 43-nt introns (schematically shown on the top) and their splicing was examined with or without the splicing inhibitor spliceostatin A (SSA: + and −). The spliced products were detected by RT–PCR using the indicated specific primers (arrows) and the amplified fragments were analyzed by 5% PAGE (the stars indicate the spliced products of these ultra-short introns). **(B)** *Xenopus* oocytes were microinjected with mini-gene containing the 56-nt intron (hnRNP H1) and the control 231-nt intron (AdML; [33]). The U1, U2, and U4 snRNAs were disrupted with anti-sense oligonucleotide-directed digestion in *Xenopus* oocytes (indicated by ΔU1, ΔU2, and ΔU4, respectively). RNA was extracted from the nuclear and cytoplasmic fractions (indicated by N and C, respectively), fractionated by denaturing 8% PAGE, and visualized by autoradiography.

indicated with arrow). Whereas splicing of the NDOR1 and ESRP2 pre-mRNAs generated larger discrete bands (lanes 11, 12, 15, 16; indicated with arrow), indicating that these are the lariat RNAs without their 3′ tails derived from the 76- and 73-nt intron lariats (see Fig. 1B). Because the splicing efficiency of the 49- and 43-nt introns was low (Supplementary Fig. S1), we failed to detect the corresponding lariat introns without their 3′ tails. Thus, the 56-nt intron is the smallest lariat structure we have detected to date.

3.6. G-rich splicing enhancer was identified in the NDOR1 and ESRP2 ultra-short introns

We searched for potential splicing enhancer elements that could play an important role in the efficient splicing of ultra-short introns [8,9]. We found a common G-rich 11-nt sequence, CAGGGGCTGGG, in the ultra-short introns of NDOR1 and ESRP2 (Fig. 4A and B, underlined). We also noticed four and three copies of the (A/T)GGG motif in the NDOR1 and ESRP2 ultra-short introns, respectively (ND1, 2 and ES1, 2, 3 in Fig. 4). Intriguingly, these G-rich elements share sequence with the known intronic splicing enhancers (ISEs), (A/T)GGG and GGGCTG motifs, which have already been identified and characterized [19,24–26].

To examine whether these G-rich sequences in the ultra-short introns promote their splicing, we introduced mutations into the (A/T)GGG motifs (Fig. 4; mutated nucleotides are indicated). The mutations in ND1 caused a clear defect in the splicing of both the 76- and 49-nt introns in the NDOR1 pre-mRNA (Fig. 4A). Interestingly, the mutations in ND2 moderately inhibited the splicing of the 76-nt intron, whereas the 49-nt intron splicing was somewhat stimulated. When we mutated the ND2 sequence more extensively

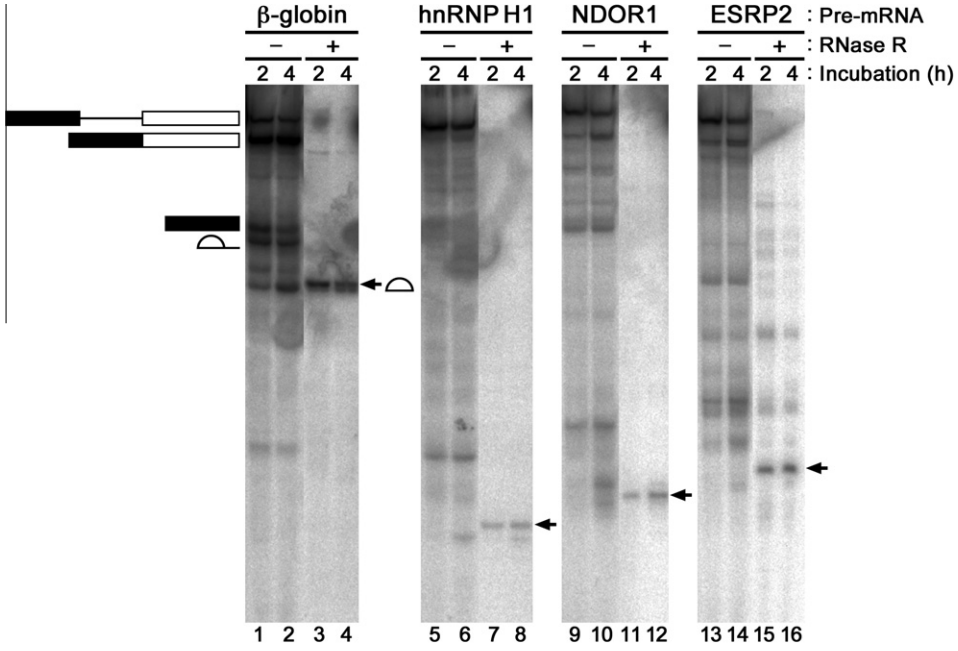

Fig. 3. Lariat structure of the 56-nt intron was identified by *in vitro* splicing. The control β-globin pre-mRNA (with a 158-nt intron) and three pre-mRNAs (with ultra-short introns) were spliced *in vitro* for the indicated incubation times (RNase R −), and the RNA products were further digested with RNase R (RNase R +). The RNAs were fractionated by denaturing 7% PAGE and visualized by autoradiography. The positions of the splicing products and RNase-digested products of the control β-globin pre-mRNA are indicated schematically with their structures. The lariat introns lacking their 3′ tails are indicated with arrows.

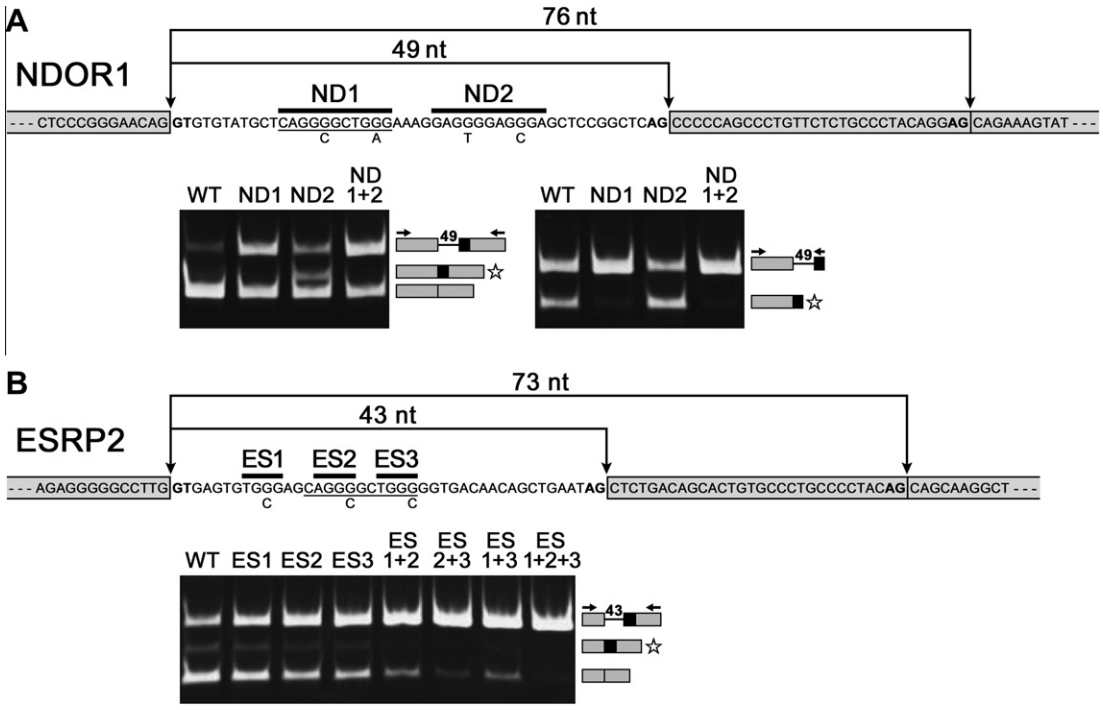

Fig. 4. Intronic G-rich elements are required to splice the NDOR1 and ESRP2 ultra-short introns. (A and B) The sequences of the NDOR1 and ESRP2 ultra-short introns and their flanking exons (shaded box) are shown. The characteristic G-rich elements (termed ND1, ND2, ES1, ES2, and ES3) were mutated with the nucleotides indicated below the sequences. The conserved 11-nt G-rich sequences shared in both NDOR1 and ESRP2 are underlined. The MCF7 cells were transfected with the mini-genes containing combinatorial mutations in the indicated G-rich elements, and the spliced products were detected by RT–PCR using the indicated specific primers (arrows). The amplified fragments were analyzed by 5% PAGE (the stars indicate the spliced products of the 49- and 43-nt introns).

(AGGGGAGGG to ACTTGACCT), the splicing of the 49-nt intron was further stimulated (data not shown). The ND2 sequence might be a specific splicing silencer for the 49-nt intron. Combined mutations in both ND1 and ND2 had an inhibitory effect essentially equivalent to that of the ND1 mutation. These data suggest that the ND1 element functions as an ISE for splicing of the 49- and 76-nt introns of the NDOR1 pre-mRNA.

In the ESRP1 pre-mRNA, the mutation in the ES1 caused a weak splicing defect for the 43- and 73-nt introns, whereas mutations in either ES2 or ES3 showed stronger splicing inhibition for both of these introns. The combined mutations showed additive effects on the inhibition of splicing, which were then especially evident when the ES1, ES2, and ES3 were fully mutated. These results indicate that ES2 and ES3 play an ISE role in the splicing of the 43- and 73-nt introns of ESRP2 pre-mRNA. Notably, the combined sequence, ES2 plus ES3, is homologous to the ND1 motif that acts as an ISE in NDOR1.

We conclude that the consensus sequence CAGGGGCTGGG functions as an ISE for the splicing of ultra-short introns in both NDOR1 and ESRP2 pre-mRNAs.

4. Discussion

Here, we report the first identification and characterization of *bona fide* ultra-short human introns (56, 49, and 43 nt) in the *HNRNPH1*, *NDOR1*, and *ESRP2* genes, respectively. The functional proteins NDOR1 (diflavin oxidoreductase) and ESRP2 (epithelial splicing regulatory protein) are produced by the use of the distal 3′ splice sites in their pre-mRNAs. Utilization of the proximal 3′ splice site of NDOR1 (excision of the 49-nt intron) generates a protein isoform (NDOR1_v1) with a 90% reduction in its reductase activity [27]. Utilization of the proximal 3′ splice site of ESPR2 (excision of 43-nt intron) potentially generates a protein with altered activity (because the intronic 30-nt insertion is in-frame). The diflavin reductase encoded by NDOR1 (also known as NR1) is highly expressed in cancer cell lines, and plays a potential role in the activation of anti-cancer drugs [28]. The ESRP2 protein controls the alternative splicing of the fibroblast growth factor receptor 2 pre-mRNA to produce the epithelial cell-type isoform, which can contribute to the process of cancer metastasis [29]. Therefore, the alternative splicing of these ultra-short introns (49 and 43 nt) might be involved in regulating the process of cancer progression.

Because steric hindrance on the ultra-short intron might be caused by the binding of essential spliceosomal components, we postulate that these ultra-short introns are spliced with fewer components than those in the authentic spliceosome. This scenario is supported by the observation in *Drosophila* that the structure of the spliceosomal B complex that formed on a short intron (62 nt) is more compact than that formed on a long (147 nt) intron. Notably, a smaller head domain, which contained the main components of the early A complex, was observed in the spliceosome that associated with the short intron [30]. We found that SF3b, at least, was necessary for splicing of all the ultra-short introns tested, but we have not yet examined the dispensability of any U snRNAs in splicing of the shorter two introns (43 and 49 nt). We are planning to undertake a comprehensive analysis, using mass spectrometry, of the spliceosomal proteins that are associated with the ultra-short introns.

Remarkably, we obtained evidence suggesting that the ultra-short introns recruit specific factors that are not the normal components of the authentic spliceosome. We have demonstrated that the consensus G-rich sequence of NDOR1 and ESRP2, CAGGGGCUGGG, is important for splicing of their 49- and 43-nt introns, respectively. This consensus element shares sequence with previously characterized ISE, GGGCUG, found in the chicken cardiac troponin T pre-mRNA, which is recognized by SF1 and is necessary for the inclusion of a 6-nt adjacent exon (termed micro-exon) in the mRNA [25,31].

It has been reported that the frequency of the GGG triplet is significantly higher than that of any other nucleotide-triplet in human short introns with lengths of less than 200 nt [26], which is also true of the selected ultra-short introns with lengths of less than 56 nt (Supplementary Table S1). Because ~2/3 of the selected ultra-short introns are G-rich and they have neither apparent branch-site sequences nor polypyrimidine tracts (Supplementary Table S1), the G-rich ISEs could be critical signals for their identification as introns. To search for the *trans*-acting factors that interact with these G-rich ISEs is underway. Interestingly, the GGG triplet interacts with U1 snRNP *via* non-canonical base pairing with the U1 snRNA, and stimulates SR protein-independent splicing at the upstream 5′ splice site [32].

In contrast, the splicing of the 56-nt intron, which contains an apparent branch site and polypyrimidine sequences, could be facilitated by a possible exonic splicing enhancer (ESE) in its flanking exons because splicing of the 56-nt intron was repressed when it was inserted into the heterologous exons (Supplementary Fig. S2).

In summary, a G-rich ISE-mediated mechanism is required for the splicing of the 49- and 43-nt ultra-short introns, which is distinct from the rather conventional splicing pathway of the 56-nt ultra-short intron that requires the conventional U snRNPs.

Acknowledgments

We are grateful to Drs. M. Yoshida and A. Malhotra for providing the spliceostatin A and the purified recombinant RNase R, respectively. We thank Drs. A.R. Krainer and R. Yoshimoto for their valuable suggestions, and members of our laboratory for their support and discussions. This work was funded by research grants from the Hori Information Science Promotion Foundation to N.S-H. and the Okawa Foundation for Information and Telecommunications to A.M.

Appendix A. Supplementary data

Supplementary data associated with this article can be found, in the online version, at http://dx.doi.org/10.1016/j.bbrc.2012.05.112.

References

[1] L.P. Lim, C.B. Burge, A computational analysis of sequence features involved in recognition of short introns, Proc. Natl. Acad. Sci. USA 98 (2001) 11193–11198.
[2] J. Zhu, F. He, D. Wang, et al., A novel role for minimal introns: routing mRNAs to the cytosol, PLoS One 5 (2010) e10144.
[3] S.M. Berget, Exon recognition in vertebrate splicing, J. Biol. Chem. 270 (1995) 2411–2414.
[4] A.J. Matlin, M.J. Moore, Spliceosome assembly and composition, Adv. Exp. Med. Biol. 623 (2007) 14–35.
[5] C.L. Will, R. Lührmann, Spliceosome structure and function, Cold Spring Harb. Perspect. Biol. 3 (2011) a003707.
[6] B. Wieringa, E. Hofer, C. Weissmann, A minimal intron length but no specific internal sequence is required for splicing the large rabbit β-globin intron, Cell 37 (1984) 915–925.
[7] P.J. Ulfendahl, U. Pettersson, G. Akusjarvi, Splicing of the adenovirus-2 E1A 13S mRNA requires a minimal intron length and specific intron signals, Nucleic Acids Res. 13 (1985) 6299–6315.
[8] Z. Wang, C.B. Burge, Splicing regulation: from a parts list of regulatory elements to an integrated splicing code, RNA 14 (2008) 802–813.
[9] W.F. Mueller, K.J. Hertel, RNA elements involved in splicing, in: S. Stamm, C. Smith, R. Lührmann (Eds.), Alternative pre-mRNA splicing: Theory and protocols, Wiley-Blackwell, Weinheim, Germany, 2012, pp. 21–31.
[10] M.C. Wahl, C.L. Will, R. Lührmann, The spliceosome: Design principles of a dynamic RNP machine, Cell 136 (2009) 701–718.
[11] N. Behzadnia, M.M. Golas, K. Hartmuth, et al., Composition and three-dimensional EM structure of double affinity-purified, human prespliceosomal A complexes, EMBO J. 26 (2007) 1737–1748.
[12] R.E. Dickerson, H.R. Drew, B.N. Conner, et al., The anatomy of A-, B-, and Z-DNA, Science 216 (1982) 475–485.
[13] H. Niwa, K. Yamamura, J. Miyazaki, Efficient selection for high-expression transfectants with a novel eukaryotic vector, Gene 108 (1991) 193–199.
[14] R. Das, Z. Zhou, R. Reed, Functional association of U2 snRNP with the ATP-independent spliceosomal complex E, Mol. Cell 5 (2000) 779–787.
[15] Z. Zhou, J. Sim, J. Griffith, et al., Purification and electron microscopic visualization of functional human spliceosomes, Proc. Natl. Acad. Sci. USA 99 (2002) 12203–12207.
[16] D. Kaida, H. Motoyoshi, E. Tashiro, et al., Spliceostatin A targets SF3b and inhibits both splicing and nuclear retention of pre-mRNA, Nat. Chem. Biol. 3 (2007) 576–583.
[17] A. Mayeda, A.R. Krainer, In vitro splicing assays, in: S. Stamm, C. Smith, R. Lührmann (Eds.), Alternative pre-mRNA splicing: Theory and protocols, Wiley-Blackwell, Weinheim, Germany, 2012, pp. 320–329.
[18] H. Suzuki, Y. Zuo, J. Wang, et al., Characterization of RNase R-digested cellular RNA source that consists of lariat and circular RNAs from pre-mRNA splicing, Nucleic Acids Res. 34 (2006) e63.
[19] N. Mabuchi, K. Masuyama, M. Ohno, Immunoprecipitation analysis to study RNA-protein interactions in Xenopus oocytes, Methods Mol. Biol. 488 (2008) 257–265.
[20] Z.Q. Pan, H. Ge, X.Y. Fu, et al., Oligonucleotide-targeted degradation of U1 and U2 snRNAs reveals differential interactions of simian virus 40 pre-mRNAs with snRNPs, Nucleic Acids Res. 17 (1989) 6553–6568.
[21] S.A. Gerbi, A.V. Borovjagin, F.E. Odreman, et al., U4 snRNA nucleolar localization requires the NHPX/15.5-kD protein binding site but not Sm protein or U6 snRNA association, J. Cell Biol. 162 (2003) 821–832.
[22] M. Ohno, A. Segref, S. Kuersten, et al., Identity elements used in export of mRNAs, Mol. Cell 9 (2002) 659–671.
[23] K. Gao, A. Masuda, T. Matsuura, et al., Human branch point consensus sequence is yUnAy, Nucleic Acids Res. 36 (2008) 2257–2267.
[24] P. Sirand-Pugnet, P. Durosay, E. Brody, et al., An intronic (A/U)GGG repeat enhances the splicing of an alternative intron of the chicken β-tropomyosin pre-mRNA, Nucleic Acids Res. 23 (1995) 3501–3507.
[25] T. Carlo, D.A. Sterner, S.M. Berget, An intron splicing enhancer containing a G-rich repeat facilitates inclusion of a vertebrate micro-exon, RNA 2 (1996) 342–353.
[26] A.J. McCullough, S.M. Berget, G triplets located throughout a class of small vertebrate introns enforce intron borders and regulate splice site selection, Mol. Cell. Biol. 17 (1997) 4562–4571.
[27] R.D. Finn, M. Wilkie, G. Smith, et al., Identification of a functionally impaired allele of human novel oxidoreductase 1 (NDOR1), NDOR1*1, Pharmacogenet. Genomics 15 (2005) 381–386.
[28] M.J. Paine, A.P. Garner, D. Powell, et al., Cloning and characterization of a novel human dual flavin reductase, J. Biol. Chem. 275 (2000) 1471–1478.
[29] C.C. Warzecha, T.K. Sato, B. Nabet, et al., ESRP1 and ESRP2 are epithelial cell-type-specific regulators of FGFR2 splicing, Mol. Cell 33 (2009) 591–601.
[30] N. Herold, C.L. Will, E. Wolf, et al., Conservation of the protein composition and electron microscopy structure of Drosophila melanogaster and human spliceosomal complexes, Mol. Cell. Biol. 29 (2009) 281–301.
[31] T. Carlo, R. Sierra, S.M. Berget, A 5′ splice site-proximal enhancer binds SF1 and activates exon bridging of a microexon, Mol. Cell. Biol. 20 (2000) 3988–3995.
[32] A.J. McCullough, S.M. Berget, An intronic splicing enhancer binds U1 snRNPs to enhance splicing and select 5′ splice sites, Mol. Cell. Biol. 20 (2000) 9225–9235.
[33] L. Pellizzoni, N. Kataoka, B. Charroux, et al., A novel function for SMN, the spinal muscular atrophy disease gene product, in pre-mRNA splicing, Cell 95 (1998) 615–624.